Electronic Correlation in Anion *p* Orbitals Impedes Ferromagnetism due to Cation Vacancies in Zn Chalcogenides

J. A. Chan, Stephan Lany, and Alex Zunger

National Renewable Energy Laboratory, Golden, Colorado 80401, USA
(Received 7 May 2009; published 2 July 2009)

Electronic correlation effects, usually associated with open *d* or *f* shells, have so far been considered in *p* orbitals only sporadically for the localized $2p$ states of first-row elements. We demonstrate that the partial band occupation and the metallic band-structure character as predicted by local density calculations for II-VI materials containing cation vacancies is removed when the correct energy splitting between occupied and unoccupied *p* orbitals is recovered. This transition into a Mott-insulating phase dramatically changes the structural, electronic and magnetic properties along the entire series (ZnO, ZnS, ZnSe, and ZnTe), and impedes ferromagnetism. Thus, important correlation effects due to open *p* shells exist not only for first-row ($2p$) elements, but also for much heavier anions like Te ($5p$).

In compounds with partially filled *d*- or *f*-electron shells, electron correlation can determine crucially the structural, electronic, and magnetic properties, and often leads to a Mott-insulating phase despite the partial band filling [1,2]. Correlation effects are also known for the localized $2p$ orbitals of first-row anions like N or O, where they may play a role for the recently discussed topic of defect-induced magnetism without *d* elements in semiconductors [3–5]. Density functional theory (DFT) calculations based on local or semilocal functionals are widely employed to predict magnetism by cation vacancies [6–9], by first-row ($2p$) dopants [6,9,10], or by under-coordinated anions at the surface or in nanostructures [11,12]. However, it is known that these DFT approximations fail to predict the correct polaronic localization of, e.g., O-$2p$ holes, and the associated Jahn-Teller-like structural distortion [4,13,14], calling their reliability for the prediction of ferromagnetic interactions into question [4]. In the present Letter, we investigate the electronic and magnetic properties of cation vacancies along the prototypical series of binary Zn chalcogenides ZnO, ZnS, ZnSe, and ZnTe in the zinc blende structure using a recently developed theory [14] that restores the correct energy splitting between occupied and unoccupied states, and that is able to recover the hole localization and Jahn-Teller-like structural distortions without empirical input. We show that throughout the chalcogenide series the metallic band structure of the host + defect system predicted by the conventional local density or generalized gradient approximations (LDA or GGA) is changed into an insulator-type band structure analogous to the situation in a Mott insulator. Thus, important correlation effects for *p* electrons are not limited to $2p$ first-row anions, but exist also in less localized anion-*p* orbitals like the $5p$ shell of Te.

Approach.—The correct prediction of metallic vs insulating behavior requires that the energy splitting between occupied and unoccupied states is accurately described. Since (semi-) local DFT functionals generally underesti-

mate this splitting, they often incorrectly favor the metallic situation where the gap is overcome by the band dispersion (i.e., $U < W$). In order to restore the correct wave-function localization of acceptor-bound polarons, we have recently [14] introduced a hole-state potential operator of the form

$$\hat{V}_{\text{hs}} = \lambda_{\text{hs}}(1 - n_{m,\sigma}/n_{\text{host}}), \qquad (1)$$

which acts to increase the splitting between occupied and unoccupied *p* states, e.g., in the O-$2p$ shell for the case of metal-site acceptors in wide-gap oxide semiconductors [14]. Here, $n_{m,\sigma}$ is the *m*-sublevel occupancy in the spin channel σ, and n_{host} is the "normal" occupancy of the defect-free host (see [15]). The present calculations are performed using the projector-augmented wave method [16], and the GGA parametrization of Ref. [17] for the underlying DFT functional.

In order to calculate the appropriate value for the parameter λ_{hs}, for which the correct splitting between the occupied and unoccupied *p* orbital energies is restored, we consider the fundamental requirement for an exact functional to yield energies $E(N)$ that are piecewise linear as a function of the continuous (fractional) electron number N [18]. Based on this requirement we formulated in Ref. [14] the condition that the electron addition energy should equal the single-particle energy of the initially unoccupied state, $E(N + 1) - E(N) = e_i(N)$, or, equivalently, that the electron removal energy should equal the single-particle energy of the initially occupied state, $E(N - 1) - E(N) = e_i(N)$. Thus, we obtain $\lambda_{\text{hs}} = 4.3$, 3.8, 3.5, and 3.1 eV, for ZnO, ZnS, ZnSe, and ZnTe, respectively. Remarkably, the strength of the correction is comparable in magnitude along the series O $\rightarrow$ S $\rightarrow$ Se $\rightarrow$ Te, and is not dramatically stronger for the first-row ($2p$) anion oxygen than for the $3p$-$5p$ chalcogen anions.

Mott-insulating phase of the II-VI host + vacancy system.—Figure 1(a) shows the density of states for a cation vacancy V_{Zn} in ZnTe, calculated in a 64 atom supercell using the standard GGA functional. The charge-neutral
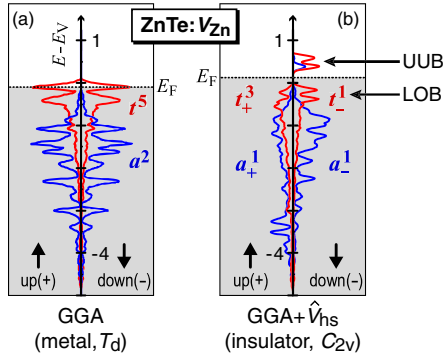
FIG. 1 (color online).   Spin-resolved local density of states for the a_1- and t_2- derived projections at the site of the Zn vacancy. Energies are given in eV relative to the ZnTe valence band maximum (E_V). The ZnTe:V_{Zn} host + defect system is predicted to be a metal in GGA (a), but becomes an insulator when the correct energy splitting between occupied and unoccupied states is recovered (b). Arrows (UUB and LOB) indicate the upper unoccupied and lower occupied (Hubbard) bands.

vacancy introduces two holes in a non-spin-polarized t_2 symmetric state at the top of the ZnTe valence band, and conserves the tetrahedral (T_d) point group symmetry. The band-structure character of the host + vacancy system is that of a non-spin-polarized metal [Fig. 1(a)]. However, the results obtained with the hole-state potential $\hat{V}_{hs}$ draw an entirely different physical picture: As shown in Fig. 1(b), the previously non-spin-polarized and partially filled t_2 symmetric band at the Fermi level [see Fig. 1(a)] now becomes spin polarized where the majority spin direction is fully occupied ($a_+^1 t_+^3$), and the minority spin accommodates the two holes ($a_-^1 t_-^1$), leading to a high-spin (HS, $S = 1$) state. More importantly, the minority t_- level splits further into one lower-energy occupied and two higher-energy unoccupied subbands (i.e., lower and upper Hubbard bands), thereby opening a gap, in direct analogy to the Mott transition [Fig. 1(b)]. A low-spin (LS, $S = 0$) state with a $a_+^1 a_-^1 t_+^2 t_-^2$ configuration, which is also insulating, lies only slightly higher in energy. (For ZnO, ZnS, and ZnSe, GGA finds a spin-polarized state of V_{Zn}^0, but the level splitting occurs only in the presence of the potential $\hat{V}_{hs}$.)

The results of the present calculations for V_{Zn} are summarized in Table I.

The complex energy surface of V_{Zn}.—Because of a Jahn-Teller distortion, the symmetry of V_{Zn}^0 is reduced to C_{2v} in the insulating phase, as schematically illustrated in Fig. 2. The distances of the ligand anions from the vacancy center for the lowest energy configurations of V_{Zn} are given in Table I. While standard LDA or GGA calculations do find a spin-polarized vacancy state for the case of the more localized $2p$ orbitals of ZnO [9] and GaN [8], they do not describe the symmetry breaking and the splitting of a partially occupied band into full and empty subbands. In contrast, our calculated spin densities for the HS and LS states of V_{Zn}^0, shown in Figs. 3(a) and 3(b), respectively, for ZnTe, demonstrate the localization at only two out of the four previously equivalent ligands [the local magnetic moments are 0.8, 0.6, 0.6, 0.5 μ_B for O, S, Se, and Te within the respective integration radii of 1.0, 1.0, 1.1, and 1.2 Å]. The metal-to-insulator transition upon application of $\hat{V}_{hs}$ occurs for V_{Zn} in all Zn chalcogenides studied. However, it is an interesting observation that in ZnO the symmetry breaking and insulating behavior is entirely electronically driven; i.e., it occurs even without any lattice distortion, whereas in the other II-VI's the electronic symmetry breaking occurs only when the structural distortion is allowed.

Indeed, we observe complex energy surfaces for V_{Zn} in Zn-VI semiconductors (Fig. 2), which are not revealed by standard DFT calculations. In the HS state of V_{Zn}^0, a T_d symmetric configuration exists as a metastable minimum in all Zn-VI's but ZnO; i.e., it is locally stable even without enforcing the constraint of T_d symmetry (Table I). Only in ZnO, the barrier $\Delta E_{b\text{-HS}}$ vanishes. The spin density of this locally stable symmetric configuration is equally distributed over all four ligands [see Fig. 3(c)] and is significantly farther extended than that of the C_{2v} symmetric ground state, but it is more localized than the spin density in a standard GGA calculation (when calculated in ZnTe with a fixed spin moment constraint). In case of the LS state of V_{Zn}^0 a similar local minimum with near-T_d symmetry (see Fig. 2) exists, but this time the barrier $\Delta E_{b\text{-LS}}$ exists only in ZnTe, but not in ZnO, ZnS, and ZnSe.

TABLE I.   Properties of neutral and charged Zn vacancies in Zn-VI semiconductors: The energy gain $\Delta E_{T_d\text{-}C_{2v}}$ (V_{Zn}^0) and $\Delta E_{T_d\text{-}C_{3v}}$ (V_{Zn}^-) due to the Jahn-Teller type symmetry breaking (relative to a constrained T_d symmetric calculation), the distances d_1 and d_2 from the vacancy center for the anions with and without a trapped hole, respectively, the energy difference $\Delta E_{LS\text{-}HS}$ between the high-spin (HS, $S = 1$) and low-spin (LS, $S = 0$) states of V_{Zn}^0, and the first and second acceptor ionization energies $\varepsilon(0/-)$ and $\varepsilon(-/2-)$.

	V_{Zn}^0 (2 holes)			V_{Zn}^- (1 hole)		V_{Zn}^{2-} (0 holes)		
	$\Delta E_{T_d\text{-}C_{2v}}$ [eV]	d_1/d_2 [Å]	$\Delta E_{LS\text{-}HS}$ [meV]	$\Delta E_{T_d\text{-}C_{3v}}$ [eV]	d_1/d_2 [Å]	d_2 [Å]	$\varepsilon(0/-)$ [eV]	$\varepsilon(-/2-)$ [eV]
ZnO	0.58	2.32/2.06	1	0.47	2.31/2.15	2.19	0.95 (1.28[a])	1.25 (1.59[a])
ZnS	0.25[b]	2.60/2.22	5	0.26	2.58/2.26	2.29	0.48	0.82
ZnSe	0.19[b]	2.72/2.29	5	0.21	2.71/2.33	2.35	0.38	0.67
ZnTe	0.07[b]	2.89/2.44	9	0.09[b]	2.89/2.48	2.51	0.17	0.41

[a]Based on GGA + U(Zn-d).
[b]T_d symmetric configuration is locally stable due to an energy barrier.
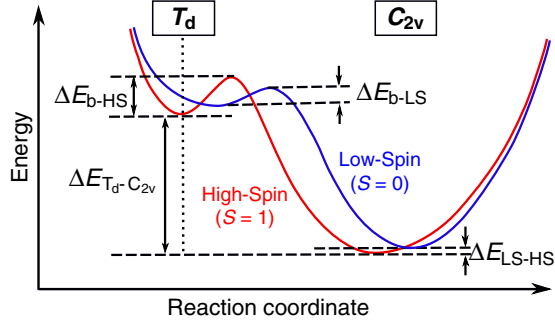
FIG. 2 (color online).   Schematic Born-Oppenheimer energy surface for the high-spin ($S = 1$) and low-spin ($S = 0$) states of the neutral V_{Zn} in Zn-VI semiconductors. The reaction coordinate points into the direction of the symmetry breaking Jahn-Teller mode (C_{2v}).

So far, we discussed only the charge neutral state V_{Zn}^0 which has two holes bound to V_{Zn} [see Figs. 3(a)–3(c)]. However, V_{Zn} can also exist in a singly charged V_{Zn}^- ($S = \frac{1}{2}$) state with one hole bound [Fig. 3(d)], and in the fully ionized state V_{Zn}^{2-} without any bound holes. In case of the singly charged vacancy V_{Zn}^-, the lowest energy configuration has a large trigonal (C_{3v}) distortion [see Fig. 3(d)], and a locally stable near-T_d configuration exists in ZnTe (Table I). As discussed further below, the complexity of the energy surface could have important implications for magnetism due to partially filled p orbitals. In case of the fully ionized state V_{Zn}^{2-} the anion-p shell is closed, and there is no Jahn-Teller effect (Table I); i.e., the T_d point group symmetry is preserved.

Comparison of V_{Zn} in ZnSe with experiment.—Since the quantitative prediction (without empirical parameter ad-
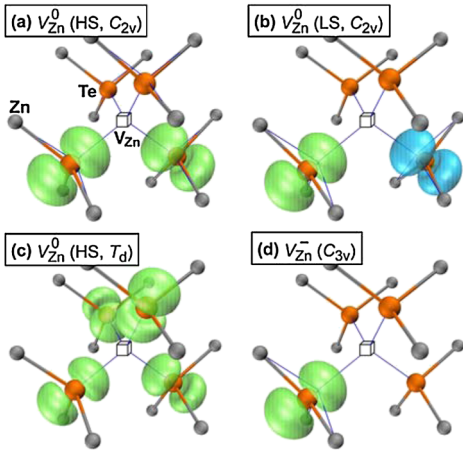
FIG. 3 (color online).   The calculated spin densities for V_{Zn} in Zn-VI semiconductors. Shown is the isosurface ($\pm 0.03 \mu_B/\text{Å}^3$) for ZnTe, but V_{Zn} in the other Zn-VI's is qualitatively very similar. (a) V_{Zn}^0 in the C_{2v} symmetric high-spin (HS, $S = 1$) state and (b) in the respective low-spin (LS, $S = 0$) state. (c) The locally stable T_d symmetric configuration of V_{Zn}^0. (d) The C_{3v} symmetric V_{Zn}^- ($S = \frac{1}{2}$). The solid (blue) lines show the unrelaxed zinc blende lattice.

justment) of acceptor binding energies is more challenging than just getting the correct hole localization and Jahn-Teller distortion [14], we now validate our predictions for the experimentally well-characterized case of V_{Zn} in ZnSe [19]: First of all, the C_{3v} symmetric configuration of V_{Zn}^- with one hole being localized at just one Se neighbor [Fig. 3(d)], now agrees with the qualitative picture obtained from the electron paramagnetic resonance characterization, which was not the case in previous LDA calculations [20]. Further, Watkins *et al.* [19] determined the optical (vertical) transition from V_{Zn}^- to V_{Zn}^{2-} as 1.75 eV relative to the conduction band minimum [i.e., 1.07 eV relative to the valence band minimum (VBM)] and the reverse transition from V_{Zn}^{2-} to V_{Zn}^- as 2.51 eV (0.31 eV relative to the VBM), amounting to a Stokes shift of 0.76 eV. In very close agreement, we calculate the respective transitions at 1.10 eV and 0.45 eV relative to the VBM (Stokes shift of 0.65 eV). Also, our calculated second acceptor ionization energy at 0.67 eV (Table I) agrees very well with the experimental value of 0.66 eV [19]. Thus, our method not only restores the qualitative correct symmetry and localization of holes at individual anion ligands, but also allows quantitative predictions for acceptor energies. As shown in Table I, acceptor levels that were found very close to the VBM in conventional DFT calculations now lie deep inside the band gap. In ZnO, where the strong p-d repulsion considerably affects the energy of the VBM, we determined the acceptor levels $\varepsilon(0/-)$ and $\varepsilon(-/2-)$ also in a calculation based on GGA + U ($U_{Zn\text{-}d} = 6$ eV), which should give more accurate acceptor energies [21]. In the other Zn-VI semiconductors, GGA + $U_{Zn\text{-}d}$ has only a small effect.

Magnetic coupling of vacancy pairs.—Standard GGA calculations in ZnO, in which the hole–wave function is incorrectly distributed over all four O neighbors, sustained considerable ferromagnetic coupling energies for V_{Zn}-V_{Zn} pairs over large distances. For example, the difference between the ferromagnetic (FM) and antiferromagnetic (AF) configurations of two V_{Zn} in their high-spin ($S = 1$) states, separated by 4.6 and 8.4 Å was determined in Ref. [9] as $\Delta E_{\text{AF-FM}} = 16$ and 32 meV, respectively. For direct comparison, we calculated the same vacancy pairs, which have a larger distance than the nearest neighbor (NN) pairs, in wurtzite ZnO, finding $\Delta E_{\text{AF-FM}} < 1$ meV in both cases; i.e., the coupling is essentially eliminated after the holes are allowed to localize at single ligands. Thus, corroborating the conclusion of Ref. [4], we emphasize that magnetic coupling between defects can be reliably predicted only by theories that correctly describe the wavefunction localization of the individual defects. Since spin-polarized surface states like those found in LDA for the O-terminated (0001) ZnO surface [11] or for nanocrystals of ZnO [12] originate from partially filled p orbitals due to undercoordinated O atoms, akin to the ligands of the cation vacancies, the prediction of such magnetic surface properties using standard (semi-)local DFT functionals probably

| | E(S)−E(S=2) [meV] | |
	S=1	S=0
ZnO	4	7
ZnS	11	22
ZnSe	9	23
ZnTe	10	34
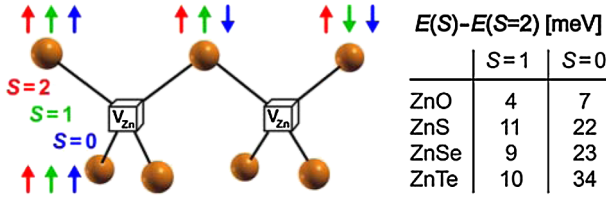
FIG. 4 (color online).   Left: Schematic illustration of the lowest energy configurations for the 1st NN pair V_{Zn}-V_{Zn} in the different spin states ($S = 2, 1, 0$). Right: The energies of the lower spin states relative to the high-spin ground state.

experiences similar difficulties as in case of the cation vacancy pair interaction.

Regarding the magnetic coupling between NN pairs of vacancies, we face here a much more complex situation than in conventional systems, like GaAs:Mn, where one needs to compare only two (FM and AF) configurations. Since, as illustrated in Fig. 4, the two vacancies on the cation sublattice share a common anion that mediates the magnetic interaction between the vacancies, one might rather view the NN vacancy pair as a single entity, where there are four holes that can be distributed over seven ligands, and the spin configurations can couple to a total spin of $S = 2, 1,$ and 0. Figure 4 shows schematically the spin distribution and relative energies for the different spin states in the respective configurations that we found to be lowest in energy. We see that the highest spin ($S = 2$) state is stabilized by up to 34 meV in ZnTe, relative to the $S = 0$ state. Considering that the strongest tendency towards ferromagnetism exists for V_{Zn} in ZnTe (see Fig. 4), we further considered more distant V_{Zn} pairs in ZnTe (up to 4th NN), but found, similar to what was discussed above for ZnO, that the magnetic coupling is negligible due to the strong localization of the hole wave-function [Fig. 3(a)]. When interactions between vacancies are limited to 1st NN pairs, one requires unrealistically high (19.8%) defect concentrations to overcome the percolation threshold [7]. Thus, we conclude that cation vacancies in II-VI semiconductors present no viable route to achieve d^0 magnetism in semiconductors.

Finally, we would like to provide a speculative outlook on the feasibility of magnetism by cation vacancies in other systems: Considering that the relaxation energy $\Delta E_{T_d\text{-}C_{2v}}$ due to the Jahn-Teller effect is reduced from 0.6 eV for ZnO to 0.1 eV for ZnTe (Table I), it is conceivable that there exist other materials where $\Delta E_{T_d\text{-}C_{2v}}$ changes the sign and where the cation vacancy has the symmetric HS state (see Fig. 2 at the T_d coordinate) as the global energy minimum. This situation could considerably stabilize the HS over the LS configuration compared to the disappointingly small $\Delta E_{LS\text{-}HS}$ energy differences (Table I) in the nonsymmetric state (Fig. 2 at the C_{2v} coordinate), thereby leading to a more robust magnetic moment. Further, the metastable T_d symmetric configuration of V_{Zn}^0 in ZnTe [see Fig. 3(c)] has a longer-ranged tail of the spin density than

the symmetry-broken C_{2v} configuration, which suggests that such—so far hypothetical—cases of symmetric vacancies could sustain long-range FM interactions.

Conclusions.—We showed that electronic correlation effects beyond standard (semilocal) DFT functionals are decisive for the structural, electronic, and magnetic properties of systems involving partially filled anion-p orbitals, not only for first-row elements like O, but also for much heavier anions including Te.

[1] N. F. Mott, *Metal-Insulator Transitions* (Taylor & Francis Ltd., London, 1974).
[2] M. Imada, A. Fujimori, and Y. Tokura, Rev. Mod. Phys. **70**, 1039 (1998).
[3] I. S. Elfimov *et al.*, Phys. Rev. Lett. **98**, 137202 (2007).
[4] A. Droghetti, C. D. Pemmaraju, and S. Sanvito, Phys. Rev. B **78**, 140404(R) (2008).
[5] V. Pardo and W. E. Pickett, Phys. Rev. B **78**, 134427 (2008).
[6] K. Kenmochi *et al.*, Jpn. J. Appl. Phys. **43**, L934 (2004).
[7] J. Osorio-Guillén, S. Lany, and A. Zunger, Phys. Rev. Lett. **100**, 036601 (2008).
[8] P. Dev, Y. Xue, and P. Zhang, Phys. Rev. Lett. **100**, 117204 (2008).
[9] H. Peng *et al.*, Phys. Rev. Lett. **102**, 017201 (2009).
[10] H. Pan *et al.*, Phys. Rev. Lett. **99**, 127201 (2007).
[11] N. Sanchez, S. Gallego, and M. C. Muñoz, Phys. Rev. Lett. **101**, 067206 (2008).
[12] A. L. Schoenhalz *et al.*, Appl. Phys. Lett. **94**, 162503 (2009).
[13] G. Pacchioni *et al.*, Phys. Rev. B **63**, 054102 (2000).
[14] S. Lany and A. Zunger, arXiv:0905.0018.
[15] The technical implementation of $\hat{V}_{hs}$ is achieved through a combination of the occupation dependent LDA + U potential $\hat{V}_U = U_{eff}(\frac{1}{2} - n_{m,\sigma})$ [S. L. Dudarev *et al.*, Phys. Rev. B **57**, 1505 (1998)] and the occupation-independent nonlocal external potential $\hat{V}_{NLEP}$ [S. Lany *et al.*, Phys. Rev. B **77**, 241201(R) (2008)], both being applied to the anion-p orbitals. The specific form of $\hat{V}_{hs}$ avoids the ambiguities occurring in LDA + U due to the strong dependence of n_{host} on the projection radius [14].
[16] G. Kresse and J. Joubert, Phys. Rev. B **59**, 1758 (1999).
[17] J. P. Perdew, K. Burke, and M. Ernzerhof, Phys. Rev. Lett. **77**, 3865 (1996).
[18] J. P. Perdew *et al.*, Phys. Rev. Lett. **49**, 1691 (1982).
[19] D. Y. Jeon, H. P. Gislason, and G. D. Watkins, Phys. Rev. B **48**, 7872 (1993).
[20] S. Pöykkö, M. J. Puska, and R. M. Nieminen, Phys. Rev. B **57**, 12 174 (1998).
[21] The parameter $\lambda_{hs} = 4.5$ eV is determined for the calculation based on GGA + U. In Ref. [14] we obtained similar, but slightly deeper transition levels for V_{Zn} in wurtzite ZnO where an additional empirical band-gap correction was applied. Note also that V_{Zn} can exist in positively charged states (not discussed in the present work) when E_F is close to the VBM [14].